Journal of the Korean Crystal Growth and Crystal Technology
Vol. 15, No. 4 (2005) 135-140

Susceptor design by numerical analysis in horizontal CVD reactor

Jung Hun Lee†, Jin Bok Yoo* and So Ik Bae

R&D Center, Siltron Inc., Gumi 730-724, Korea
**CFD Solution Div., ATES, Seoul 152-848, Korea*

(Received June 28, 2005)
(Accepted July 20, 2005)

Abstract Thermal-fluid analysis was performed to understand the thermal behavior in the horizontal CVD reactor, thereby, to design a susceptor which has a uniform deposition rate during silicon EPI growing. Four different types of susceptor designs, standard (no hole susceptor), hole #1 (240 mm), hole #2 (150 mm) and hole #3 (60 mm), were simulated by CFD (Computational Fluid Dynamics) tool. Temperature, gas flow, deposition rate and growth rate were calculated and analyzed. The degree of flatness of EPI wafer loaded on the susceptor was computed in terms of silicon growth rate. The simulation results show that the temperature and thermal distribution in the wafer are greatly dependent on inner diameter of hole susceptor and demonstrate that the introduction of hole in the susceptor can degrade wafer flatness. Maximum temperature difference appeared around holes. As the diameter of the hole decreases, flatness of the wafer becomes poor. Among the threes types of susceptors with the hole, optimal design which resulted a good uniform flatness (5 %) was obtained when using hole #1.

Key words CVD (Chemical Vapor Deposition), Deposition rate, Susceptor design, CFD (Computational Fluid Dynamics), Uniform flatness

1. Introduction

CVD (Chemical Vapor Deposition) refers to the process that deposits a thin film such as silicone on the wafer surface using chemically reactive gases. CVD process is applied extensively in the high quality device industry because it produces a very uniform and defect-free epitaxial layer on top of the substrate.

During the EPI process boron gas is fed into the reactor to satisfy the target resistivity requirements. In order to prevent the auto-doping phenomenon, where the boron atom from the side and bottom of the wafer is included into the epitaxy layer, an oxide layer on the bottom of the wafer is usually used. However, the cost associated with removal of the oxide layer is becoming problematic. Lately the method of allowing free exhaust of boron gas via a hole in the susceptor is being considered. But in using the susceptor with holes, there were occurrences of abnormal EPI deposition having adverse effects on the wafer quality, especially the flatness quality. The flatness problem caused by the abnormal EPI deposition is being solved through variations of main design parameters, such as number of holes, size, and density.

For an optimal susceptor design and analysis of EPI process and the reactor, solving of equations for flow, energy, and surface chemical reaction [1-3, 9] is required. Various thermal-fluid simulation code is used for this purpose. Currently there are little research regarding susceptor with hole, and most focus on hole-less susceptor reactor's flow and isothermal analysis, mainly by Moffat [7], Fotiadis [10], Jensen [7, 10, 13], and Habuka [1-3, 9].

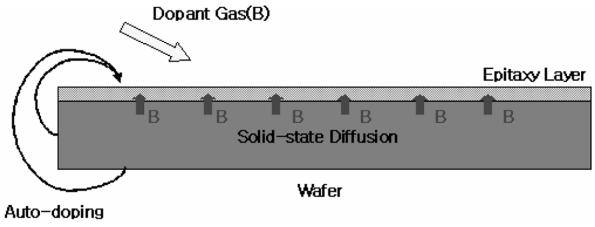

Fig. 1. Autodoping phenomena by unwanted doping, out-diffusion of boron dopant.

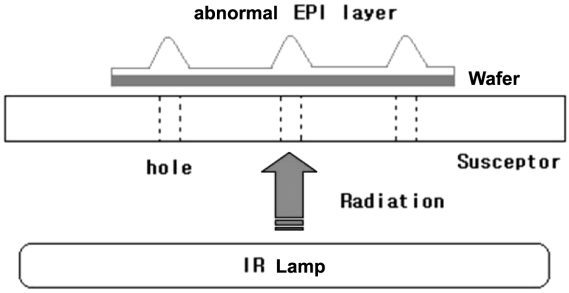

Fig. 2. Site flatness problem on the wafer by abnormal EPI deposition around hole.

†Corresponding author
Tel: +82-54-470-6257
Fax: +82-54-470-6283
E-mail: junghun@lgsiltron.co.kr

This research simulated the effects of susceptor design on the horizontal CVD reactor's flow, temperature distribution, deposition rate and growth rate, and examined the degraded flatness due to abnormal EPI deposition in susceptor with holes, and then presents the optimal susceptor design.

2. Theoretical Background

2.1. Analysis reactor geometry

Analysis subject of this research is a horizontal CVD reactor such as Fig. 3, which consists of 5 injectors, quartz wall, susceptor, susceptor ring, IR Lamp etc. Each injector feeds a pre-mixed carrier gas (H_2) and TCS ($SiHCl_3$) gas and the flow rate is adjustable. Susceptor is made of graphite with SiC coating, rotates at 35 rpm to provide a long residence time of reactive gases on the wafer surface, and allows EPI layer to grow evenly. An IR lamp exists on the outside of the reactor to maintain susceptor upper part temperature of 1,373 K (1,100°C) to satisfy chemical reaction condition of pre-mixed reactive gases. Three types of susceptor models are used in the analysis: standard, single hole and about 90-holes susceptor as in Fig. 4. Single hole susceptors which have models of 3 different types (D_i/D_o=0.8 [#1], 0.5 [#2], 0.2 [#3]) are chosen to determine temperature distribution characteristics with changes of hole diameter.

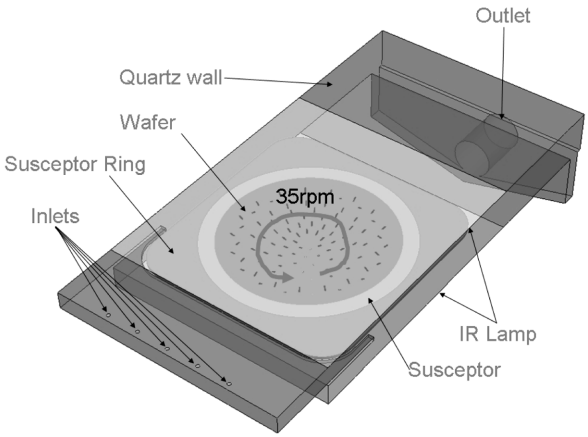

Fig. 3. Schematic of horizontal CVD reactor.

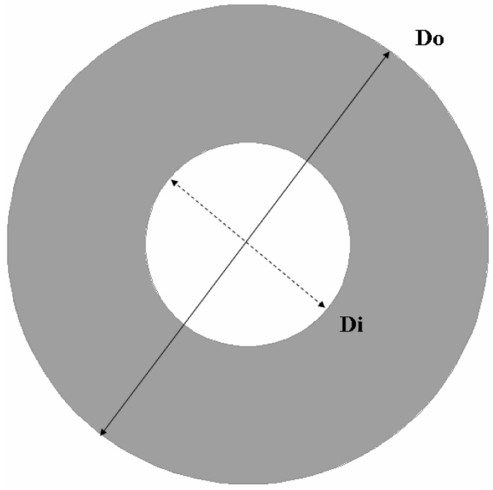

Fig. 4. Schematic of single hole susceptor.

2.2. Governing equation

This study performed calculations of reactive gas flow pattern, temperature distribution and Si growth rate within the CVD reactor. Three-dimensional mass, momentum, energy conservation equation, as well as chemical species conservation and surface reaction equation [1-3] were used. In order to perform growth rate calculations, in addition to chemical reaction, thermal-fluid field should be analyzed at the same time and Si epitaxy model equation will contain non-linear tendencies, which require much calculation times to acquire convergent solution.

The flow within the CVD reactor is a laminar flow and it is considered that diffusion due to chemical species concentration and convective phenomenon by thermal gradient cause many effects on the flow field. External forces are considered dismal and only the gravitational effects are considered. The gas mixture satisfies the ideal gas equation, and heat generation by chemical reaction is considered minimal. In this research, we calculated a convergent solution of steady-state, and all partial differential parts of time in all governing equations were removed and expressed using the third dimensional Cartesian coordinate.

Mass conservation equation is expressed as follows:

$$\frac{\partial(\rho u)}{\partial x} + \frac{\partial(\rho v)}{\partial y} + \frac{\partial(\rho w)}{\partial z} = 0 \quad (1)$$

, where u, v and w are velocities in the x-, y-, and z-axis directions, ρ is the density of the gas mixture, and the density as function of temperature can compute using the ideal gas law.

$$\rho = \frac{pMW_{av}}{RT} \quad (2)$$

, where p is the operating pressure in the reactor, MW_{av} is average molecular weight of the mixture gas, R is the ideal gas constant, and T is the temperature in the reactor.

Momentum conservation equation to calculate velocities of the flowfield can appear as follows.

$$\nabla\cdot(\rho\vec{v}\vec{v}) = -\nabla p + \rho\vec{g} + \nabla\cdot\mu\left[(\nabla\vec{v} + \nabla\vec{v}^{T}) - \frac{2}{3}(\nabla\cdot\vec{v}I)\right] \quad (3)$$

, where p and μ are the pressure and viscosity of mixture gas, and I denotes the unit vector. Viscosity of each gas can be expressed as a function of temperature but the viscosity data used in the calculation is provided by a commercial code (Fluent) which uses the kinetic theory method. Energy conservation equation to compute temperature distribution is as follows:

$$\frac{\partial}{\partial x}(\rho u c_p T) + \frac{\partial}{\partial y}(\rho v c_p T) + \frac{\partial}{\partial z}(\rho w c_p T) = \frac{\partial}{\partial x}\left(\lambda\frac{\partial T}{\partial x}\right) + \frac{\partial}{\partial y}\left(\lambda\frac{\partial T}{\partial y}\right) + \frac{\partial}{\partial z}\left(\lambda\frac{\partial T}{\partial z}\right) \quad (4)$$

, where c_p and λ are the specific heat and thermal conductivity of each gas. Specific heat data used polynomial expression of temperature that was supplied in reference [11, 12], and thermal conductivity data was calculated using kinetic theory. Temperature distribution of interior is determined by the boundary condition at the wall and the susceptor, radiation heat transfer of IR lamp, convective flow of the gas mixture, and the thermal conduction of susceptor and wafer. P1 Model provided by Fluent code was used to calculate a radiation equation. Chemistry species conservation equation of mixture gas is as follows:

$$\frac{\partial}{\partial x}(\rho u\omega_i) + \frac{\partial}{\partial y}(\rho v\omega_i) + \frac{\partial}{\partial z}(\rho w\omega_i) = \frac{\partial}{\partial x}\left(\rho D_i\frac{\partial\omega_i}{\partial x} + \rho D_i^{T}\frac{\partial \ln T}{\partial x}\right) + \frac{\partial}{\partial y}\left(\rho D_i\frac{\partial\omega_i}{\partial y} + \rho D_i^{T}\frac{\partial \ln T}{\partial y}\right) + \frac{\partial}{\partial z}\left(\rho D_i\frac{\partial\omega_i}{\partial z} + \rho D_i^{T}\frac{\partial \ln T}{\partial z}\right) \quad (5)$$

, where $D_i^T = \alpha_i\rho D_i\omega_i\omega_{H_2}$

ω_i and D_i are the mass fraction of i chemical species (i = $SiHCl_3$, H_2) and binary diffusion coefficient of i species in H_2 gas, D_i^T is the thermal diffusion coefficient in H_2 gas, α is the thermal diffusion. Binary diffusion coefficient in this calculation used polynomial formula as a function of temperature, as is reported in Kommu's paper [4].

Boundary condition of this work tried to reflect the real CVD conditions as much as possible. The flow rate of TCS was 18 g/min, H_2 was 8 g/min and each injector fed with a constant flux and injects in the vertical direction at the exit plane in plug flow form. Quartz wall's surface temperature was maintained at 750 K and interior operating pressure was 1 atm. The flow around susceptor and wall satisfies non-slip condition. Constant heat flux ($\dot{q}$ = 310,000 W/m^2) was supplied through transparent Quartz wall from an IR lamp and maintained a surface temperature of 1,373 K on the susceptor which rotates at 35 rpm. The exhaust condition was set to maintain back-pressure at zero, supposing that there is no backflow.

2.3. Surface chemical reaction

Si growth model of 2-step adsorption and desorption reaction reported by Habuka *et al*. [9] is applied to the chemical reaction mechanism on the wafer surface. In this model the reactive gas (TCS) creates $SiCl_2$ via decomposition process in gas phase. The generated gas of $SiCl_2$ is adsorbed on the wafer surface and then reacts with hydrogen gas to become solid phase of silicon. The chemical reaction equations for each of the two steps are expressed by eq. (6) and (7), and the global equation for the reaction with eq. (8).

- $SiHCl_3$ chemisorption process

$$SiHCl_3 \rightarrow {}^{*}SiCl_2 + HCl \quad (6)$$

- $Si_{<s>}$ production process

$$^{*}SiCl_2 + H_2 \rightarrow Si_{<s>} + 2HCl \quad (7)$$

- Global chemical Reaction

$$SiHCl_3 + H_2 \rightarrow Si_{<s>} + 3HCl \quad (8)$$

This study calculated Si growth rate using global chemical reaction equation which is expressed with Arrhenius equation. Si reaction velocity expression and reaction rate constant of the global reaction step are expressed in eq. (9) and (10).

$$V = k[SiHCl_3][H_2] \quad (9)$$

$$k = \frac{k_r k_{ad}}{k_{ad}[SiHCl_3] + k_r[H_2]} \quad (10)$$

, where V is growth rate of solid Si, k_r, k_{ad} are the velocity constant of each reaction step. [$SiHCl_3$], [H_2] are mole fraction of $SiHCl_3$ and H_2. Each step's reaction rate constants are referred from [1].

3. Results and Discussion

Wafer surface temperature distribution and Si growth rate were acquired through flow and thermal analysis of

the CVD reactor. This study found the optimal susceptor shape through the results of the analysis of thermal distribution and growth rate uniformity.

3.1. Temperature Distribution

Figure 6 shows the temperature distribution of the wafer surface on 4 different types of susceptors. The result for the standard type shows a non-symmetric bias of the temperature distribution to a specific direction due to the rotation of susceptor, and the phenomenon is especially notable in Hole #1. Hole #2 and #3 also shows the same effect to the much lesser degree. On #2 and #3, higher density of isothermal-lines exists in the vicinity of the hole diameter of the susceptor. This result is influenced not only by susceptor hole position or size but also by the change in heat transfer; that is chemical species flow pattern on the wafer upper surface. The results for #2 and #3 show that the hole diameter parameter has significant influence on the temperature distribution.

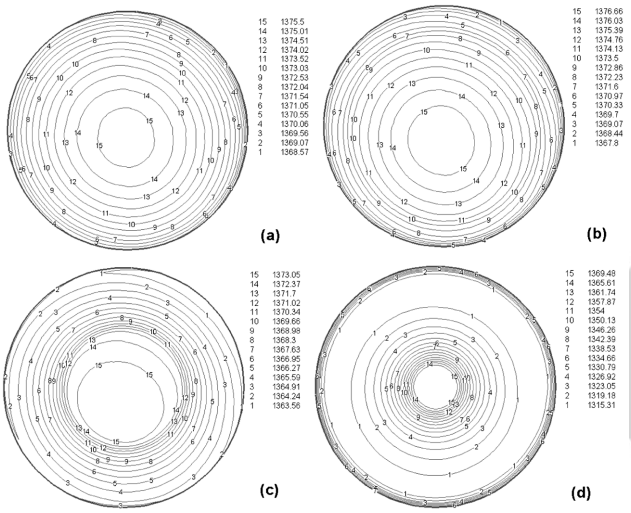

Fig. 5. Temperature distribution on the wafer surface for different types of susceptors, (a) Standard, (b) Hole #1, (c) Hole #2, (d) Hole #3.

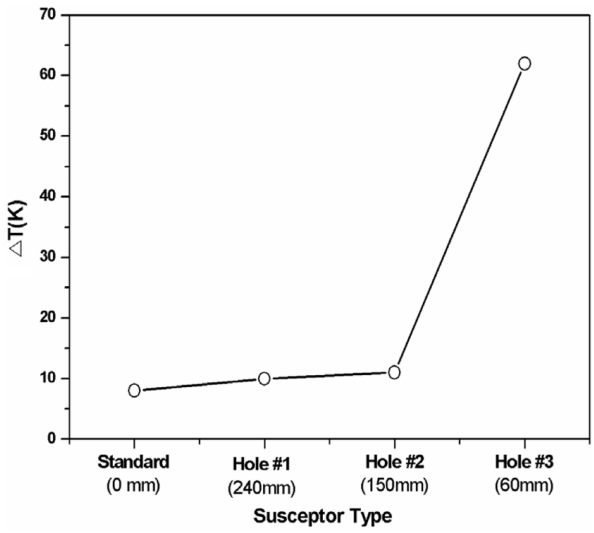

Fig. 6. Temperature difference on the wafer surface for different types of susceptors, Standard, Hole #1 (D_i = 240 mm), #2 (D_i = 150 mm) and #3 (D_i = 60 mm).

The temperature distribution on wafer surface generated by gas flow and heat transfer can be displayed in terms of the difference between maximum and minimum temperature, $\Delta T = T_{max} - T_{min}$ as in Fig. 6. The temperature difference was small, 8 K for standard, 9 K for Hole #1 and 10 K for Hole #2, while there is a much greater difference of 63 K for Hole #3.

3.2. Si deposition rate

Figure 7 shows the results of the numerical analysis of Si deposition rate. In the case of a hole-less or a large hole (Hole #1), the deposition rate was higher at near the nozzle than at the center where the temperature is high. As the hole size decreases (Hole #2, #3) the higher deposition rate region shifted to the center where the temperature is high. It is assumed that the highest deposition rate is controlled mainly by the susceptor temperature distribution, reactive gas concentration, and in-flow path, which can be shown as a product of reactive temperature and mole fraction of gases [eq. (9)].

High Si deposition rate around the hole demonstrates that the probability of abnormal EPI is high. If many small holes exist on the susceptor, then the differences

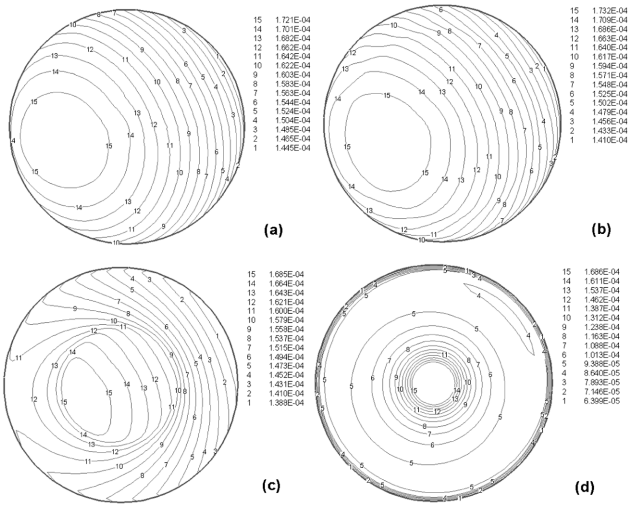

Fig. 7. Deposition rate of Si for different types of susceptors, (a) Standard, (b) Hole #1, (c) Hole #2, (d) Hole #3.

in the deposition rate can have unfavorable effects on the wafer surface flatness. On this basis, the susceptor hole diameter is judged to be a main design parameter.

3.3. Uniformity of growth rate

Flatness is one of the important issues that decide wafer's quality. The purpose of this research was to determine the causes affecting flatness and design optimal susceptor designs to provide a good uniformity of wafer thickness. Flatness level can be estimated by uniformity of growth rate, and can be expressed as the average Si deposition rate as the wafer rotates, divided by the density of solid Si. Growth rate is as follow.

$$\text{Growth rat} = V_{mean}/\rho_{Si} \quad (11)$$

The calculated result of growth rate at the centerline of wafer was depicted in Fig. 8. We can see that the center has the highest value and decreases as moved to the edge. Hole #3 shows the highest growth rate at 60 mm inner diameter, and Hole #2 shows the similar trend at 150 mm. Fig. 8 showed that the smaller size of hole caused the higher growth rate gradient between the hole area and other area, and the growth rate in the inside of hole was almost constant. As referred in research background, abnormal EPI phenomenon by hole was confirmed from the result of Hole #2 and #3. It is inferred that small diameter size hole causes the higher abnormal growth around the hole, the higher non-uniformity. To calculate the uniformity of flatness, Non-uniformity is defined as follows.

$$\text{Non-uniformity (\%)} = \frac{\text{Max}-\text{Min}}{2\times\text{Mean}}\times 100 \quad (12)$$

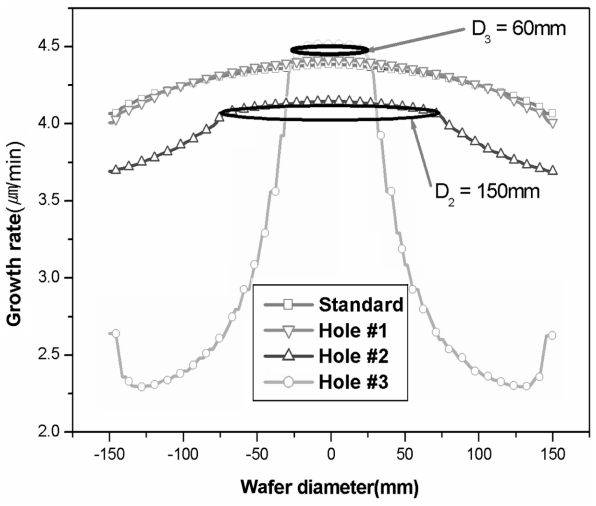

Fig. 8. Plot of growth rate for different types of susceptors.

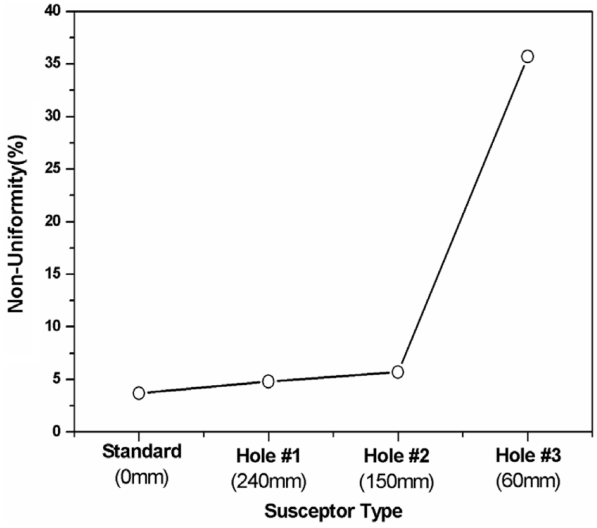

Fig. 9. Non-uniformity of the growth rate at the centerline of wafer for different types of susceptors, Standard, Hole #1 (D_i = 240 mm), #2 (D_i = 150 mm) and #3 (D_i = 60 mm).

The non-uniformity result calculated by using eq. (12) was shown in Fig. 9. It was made certain that the susceptor with highest non-uniformity level was Hole #3. As seen in Fig. 6 and 9, the results of temperature difference and non-uniformity show the similar tendency, and we can know that both results have a close correlation. The estimation of non-uniformity is possible through the result of temperature difference on wafer upper surface. In summary, Hole #1 satisfies the requirement to prevent auto-doping while providing a uniform flatness.

4. Conclusions

After analyzing the flow and the temperature distribution dependence on hole diameter, and determining growth rate uniformity, we can draw the following conclusions:

1) As the hole diameter decreases, the temperature difference at the wafer surface increases and Si deposition thickness non-uniformity increases.

2) As the hole diameter decreases, the highest Si deposition area shifts from at the nozzle to the center of the wafer where the temperature is the highest.

3) As the hole diameter decreases, growth rate gradient increases and abnormal EPI growth becomes more evident.

4) Of the three susceptor types with holes, the design with lowest non-uniformity level (5 %) was Hole #1, where the hole occupies 64 % of the wafer total surface area.

Referneces

[1] H. Habuka, *et al*., "Model on transport phenomena and epitaxial growth of silicon thin film in $SiHCl_3$-H_2 system under atmospheric pressure", J. Crystal Growth 169 (1996) 61.

[2] H. Habuka, *et al*., "Hot-wall and cold-wall environments for silicon epitaxial film growth", J. Crystal Growth 223 (2001) 145.

[3] H. Habuka, *et al*., "Formation mechanism of local thickness profile of silicon epitaxial film", J. Crystal Growth 266 (2004) 327.

[4] S. Kommu, *et al*., "A theoretical/experimental study of silicon epitaxy in horizontal single-wafer chemical vapor deposition reactors", J. Electrochem. Soc. 147 (2000) 1538.

[5] K. J. Kuijlaars, *et al*., "Muljti-component diffusion phenomena in multiple-wafer chemical vapour deposition reactors", Chem. Eng. J. 57 (1995) 127.

[6] C. R. Kleijin, *et al*., "A mathematical model of the hydrodynamics and gas-phase reactions in silicon LPCVD in a single-wafer reactor", J. Electrochem. Soc. 138 (1991) 2190.

[7] H.K. Moffat and K.F. Jensen, "Three-dimensional flow effects in silicon CVD in horizontal reactors", J. of Electrochem. Soc. 135 (1988) 459.

[8] S.V. Pantankar, "Numerical heat transfer and fluid flow", McGraw-Hill, New York (1980).

[9] H. Habuka, *et al*., "Nonlinear increase in silicon epitaxial growth rate in a $SiHCl_3$-H_2 system under atmospheric pressure", J. Crystal Growth 182 (1997) 352.

[10] D.I. Fotiadis, S. Kieda and K. F. Jensen, "Transport phenomena in vertical reactors for metalorganic vapor phase epitaxy", J. of Crystal Growth 102 (1990) 441.

[11] F.P. Incropera and D.P. DeWit, "Fundamentals of heat and mass transfer", 4th Ed. WILEY (1996).

[12] The Institution of Electrical Engineers, "Properties of SILICON", INSPEC (1988).

[13] M.L. Hitchman and K.F. Jensen, "Chemical vapor deposition", ACADEMIC PRESS (1993).